Boise State University
ScholarWorks

Electrical and Computer Engineering Faculty Publications and Presentations

Department of Electrical and Computer Engineering

10-15-2010

Cavity Resonant Mode in a Metal Film Perforated with Two-Dimensional Triangular Lattice Hole Arrays

Wan Kuang
Boise State University

Alex English
Boise State University

William B. Knowlton
Boise State University

Jeunghoon Lee
Boise State University

William L. Hughes
Boise State University

See next page for additional authors

This is an author-produced, peer-reviewed version of this article. © 2009, Elsevier. Licensed under the Creative Commons Attribution-NonCommercial-NoDerivatives 4.0 International License (https://creativecommons.org/licenses/by-nc-nd/4.0/). The final, definitive version of this document can be found online at *Optics Communications*, doi: 10.1016/j.optcom.2010.05.055

Authors
Wan Kuang, Alex English, William B. Knowlton, Jeunghoon Lee, William L. Hughes, and Bernard Yurke

This article is available at ScholarWorks: https://scholarworks.boisestate.edu/electrical_facpubs/53

NOTICE: This is the author's version of a work accepted for publication by Elsevier. Changes resulting from the publishing process, including peer review, editing, corrections, structural formatting and other quality control mechanisms, may not be reflected in this document. Changes may have been made to this work since it was submitted for publication. The definitive version has been published in Optics Communications, Vol. 283, Issue 20, Oct. 2010. DOI: 10.1016/j.optcom.2010.05.055

Cavity Resonant Mode in a Metal film Perforated with Two-Dimensional Triangular Lattice Hole Arrays

Wan Kuang[a,*], Alex English[a], Zi-Chang Chang[b], Min-Hsiung Shih[b], William B. Knowlton[a], Jeunghoon Lee[a], William L. Hughes[a], Bernard Yurke[a]

[a] *Boise State University, 1910 University Dr., Boise, ID 83725*
[b] *Research Center for Applied Science, Academic Sinica, Hsinchu, Taiwan 300*

Abstract

The transmission property of metallic films with two-dimensional hole arrays is studied experimentally and numerically. For a triangular lattice subwavelength hole array in a 150 nm thick Ag film, both cavity resonance and planar surface modes are identified as the sources of enhanced optical transmissions. Semi-analytical models are developed for calculating the dispersion relation of the cavity resonant mode. They agree well with the experimental results and full-wave numerical calculations. Strong interaction between the cavity resonant mode and surface modes is also observed.

Keywords: Surface plasmon, Metallic periodic structures

1. Introduction

The experimental finding of extraordinary optical transmission [1] through optically thick metallic films perforated with periodic arrays of subwavelength holes, or plasmonic crystals, has sparked considerable interest. Enhanced transmissions through such structures are of great scientific values and have been exploited in several nanophotonic [2] and biomedical applications [3]. Many theories have been developed to understand the mechanism of such phenomenon [4–9]. It is generally believed that the excitation and coupling of surface plasmon-polaritons (SPPs) at the planar metal-dielectric interface play an important role [4, 6, 9]. The discrete translational symmetry introduced by the hole arrays allows the coupling between the incident light and the otherwise non-radiative SPPs.

More recently, it is been numerically shown that cavity resonances can also lead to an enhanced optical transmission [5, 7, 10–12]. Several experiements have shown such behaviors in a 1D slit [13], rectangular holes [14], and annular rings [15]. The cavity resonance mechanism is based on Fabry-Pérot resonances of guided modes in the slits or holes. The quality factor of these resonances, and thus their effect on the transmission, depends on the propagation loss of the guided mode and modal reflectivity. However, questions remains as to the existence of such resonance in circular holes [15, 16]. Ordinary circular hole exhibits a very low Q factor, compared with 1D slits illuminated with p-polarized light or two dimensional 2D annular apertures with a resonant TE_{11} fundamental mode.

In this work, we numerically and experimentally demonstrated the existence of a relatively high Q cavity resonance in a triangular lattice air holes. The transmission through the cavity is resonantly enhanced at well-defined wavelengths, depending on the film thickness and the dispersion relation of the guided modes. This guided mode also differs from those in a 1D slit, a rectangular hole, or an annular ring in that the mode does not localize completely inside each circular hole. Instead, the mode is a super mode of the periodic array of holes, similar to the cladding mode of a photonic crystal fiber [17]. The work also showed that cavity resonance can strongly interact with planar surface waves, leading to an anti-crossing behavior on the transmission spectra.

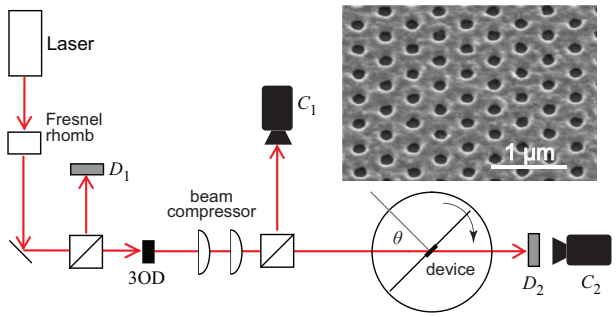

Figure 1: Scheme of the experimental setup: light from a triply-pumped Q-switch OPO laser is attenuated and compressed to a collimated 5 ns pulse with a beam diameter of 300 μm at the device surface. Using a Fresnel rhomb, the input polarization for all wavelengths of interest are maintained as linear and parallel to the plane of incidence. The inset is a scanning electron micrograph image of a plasmonic crystal.

*Corresponding author
Email address: wankuang@boisestate.edu (Wan Kuang)

NOTICE: This is the author's version of a work accepted for publication by Elsevier. Changes resulting from the publishing process, including peer review, editing, corrections, structural formatting and other quality control mechanisms, may not be reflected in this document. Changes may have been made to this work since it was submitted for publication. The definitive version has been published in Optics Communications, Vol. 283, Issue 20, Oct. 2010. DOI: 10.1016/j.optcom.2010.05.055

2. Experiments and Measurements

A number of two-dimensional arrays of cylindrical cavities in metallic films were prepared and analyzed for this study, an example of which is shown in the inset of Fig. 1. Typically, a silver film of 150 nm thick was first deposited on a Schott's N-SF6 glass substrate by physical vapor deposition. Electron beam resist, polymethyl methacrylateis (PMMA) was spin-coated and arrays of circles were exposed with electron beams. The cylindrical holes were then etched into the Ag film by ion beam etching with a subsequent removal of PMMA. The patterned area is no smaller than 300 μm $\times$ 300 μm.

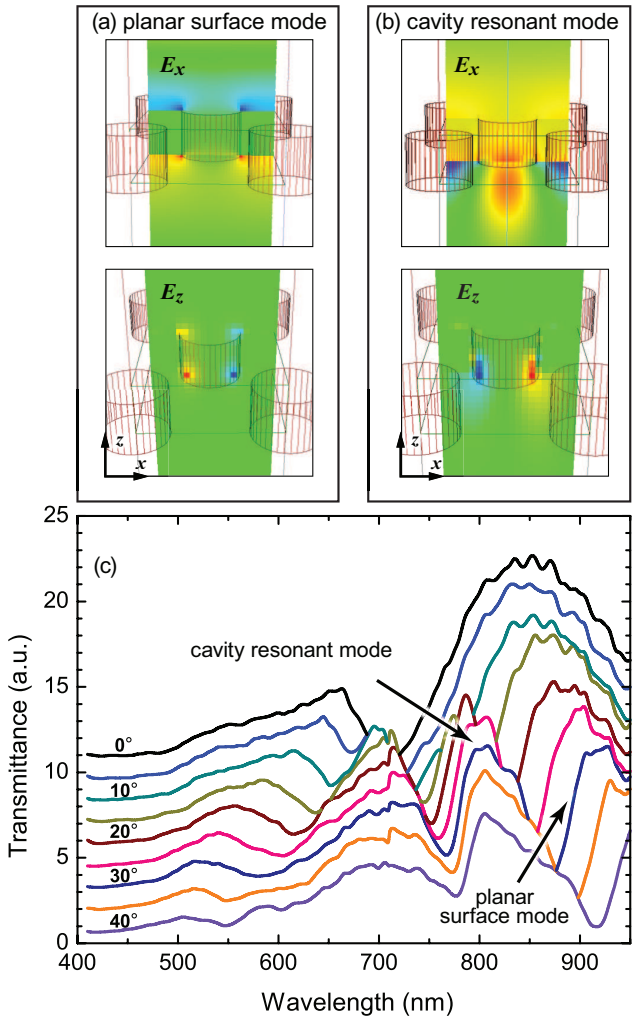

Figure 2: Calculated electric fields E_x and E_z at the wavelengths of peak transmission for 30° incidence on a 2-D periodically modified Ag film, calculated by 3-D FDTD method for (a) planar surface mode and (b) cavity resonant mode. (c) Measured optical transmission for p-wave incidence for an incident angle from 0° to 40°. A 150 nm Ag film on a glass substrate is perforated with 100 nm radius air holes in a triangular lattice. The lattice constant is 420 nm.

Figure 1 is a diagram of the system employed for optical transmission measurements. The experiments measured the transmitted power through the device as a function of incident angle, θ, and wavelength. A triply-pumped optical parametric oscillator produces a linearly polarized coherent light source that can be tuned from 420 nm to 2500 nm. The polarization for all wavelengths described in this work is parallel to the plane of incidence. The collimated beam after the beam compressor has a divergence angle of 5 mrad. The detector, D_1, measured the energy of the incoming beam and D_2 measured the energy of the transmitted beam. The attenuator, 3OD, limits the incident optical pulse energy to be less than 1 μJ, thus reduces peak incident power and eliminates the nonlinear effects.

Figure 2 shows the optical transmission of a 150 nm Ag film on an N-SF6 Schott glass substrate perforated with a triangular lattice of air holes. The lattice constant, a, is 420 nm and the radii of the air holes are 100 nm, as shown in the Fig. 1 inset. The optical transmissions of plasmonic crystals were measured for the wavelength range of 410 nm and 950 nm at a 5 nm interval. The incident angle was varied from 0° to 40° with a measurement conducted for every 5°. The transmission was taken as the ratio between the readings of the two detectors, D_2/D_1, to remove the impact of pulse-to-pulse energy fluctuation of the laser source. A measurement was also performed for the transmission of the wafer on which the device was fabricated. The response of the device was normalized by the transmittance of the wafer, eliminating the spectral response of the photodiode and the 3OD.

3. Analysis

Figure 3(a) shows the dispersion diagram of the plasmonic crystal by identifying the wavelength of peak transmissions for a given incident angle. The measurements were overlaid with the numerical results from two semi-analytical models, planar surface wave model and cavity resonance model, which represent the two mechanisms involved in enhanced optical transmissions. The purpose of these models is to identify the origin of the transmission peaks observed in Fig. 2. Since the semi-analytical model does not account for all field interactions, some differences with the the measurements are expected, particularly at the Brillouin zone boundary. However, we will show that the semi-analytical models agree qualitatively with the measurements even with these substantial approximations. A 3-D finite difference time-domain (FDTD) simulation of the dispersion relation is also shown in Fig. 3(b) as a comparison.

In the planar surface mode model, incident light couples with SPPs at the planar interface of Ag and glass. This coupling is assisted by the periodic modification of the Ag film, which scatters the incident light by one or more grating vectors to match the planar surface plasmons that is otherwise non-radiative. Under the empty lattice

NOTICE: This is the author's version of a work accepted for publication by Elsevier. Changes resulting from the publishing process, including peer review, editing, corrections, structural formatting and other quality control mechanisms, may not be reflected in this document. Changes may have been made to this work since it was submitted for publication. The definitive version has been published in Optics Communications, Vol. 283, Issue 20, Oct. 2010. DOI: 10.1016/j.optcom.2010.05.055

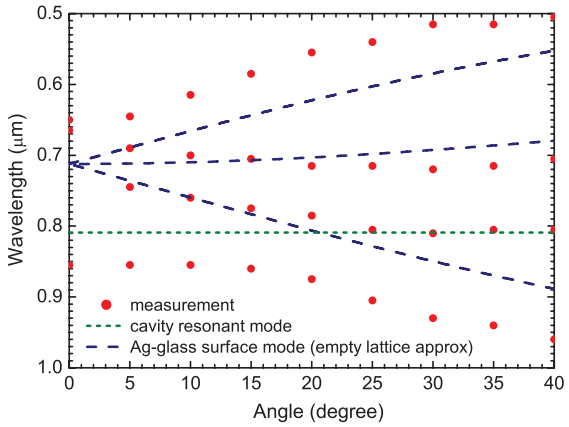

(a)

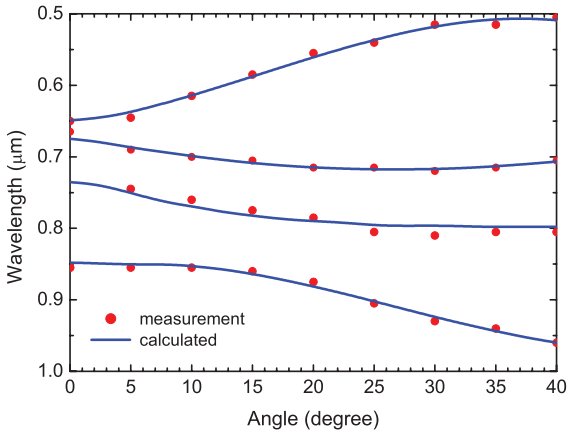

(b)

Figure 3: (a) Dispersion diagram of the 2-D periodically modified Ag film measured in Fig. 2. The circles are measured transmission peaks at a given incident angle. The dashed and dotted lines are results from semi-analytical models. (b) Dispersion diagram from the measurement, as in (a), compared with 3-D FDTD calculations.

approximation, the enhanced transmission occurs when

$$|k_0 \sin\theta \hat{x} + m\boldsymbol{b}_1 + n\boldsymbol{b}_2| = k_{SPP}, \quad m, n \in Z \qquad (1)$$

where k_{SPP} is the magnitude of the wave vector for the surface wave on the Ag-glass interface. $\boldsymbol{b}_1$ and $\boldsymbol{b}_2$ are the reciprocal lattice vectors, given by $\boldsymbol{b}_1 = \hat{y}4\pi/\sqrt{3}a$ and $\boldsymbol{b}_2 = \hat{x}2\pi/a + \hat{y}2\pi/\sqrt{3}a$ under the coordinate shown in the Fig. 2 inset. It can be seen from Fig. 3(a) that most measurements follow closely to the folded dispersion of surface modes, shown as dashed lines in the figure. And expected discrepancy is found in the vicinity of the Brillouin zone boundary, which is owing to multiple Bragg scatterings not accounted for in the empty lattice approximation.

Besides bands originated from the surface modes, a cavity resonance inside the air holes also exists around the vacuum wavelength of 809 nm, as shown by the dotted line in Fig. 3(a). This enhanced transmission is a result of Fabry-Perot interference of the waveguide mode supported along the holes of the Ag film. Similar behavior was numerically [10, 12] and experimentally [13] observed on subwavelength rectangular slits. The cavity resonance was also suggested for metal films with two-dimensional hole arrays [18]. However, the use of a perfect electric conductor (PEC) in lieu of actual metal medium in the simulations casts doubt of the generality of the result [16]. The cutoff frequency of a propagation mode for a cylindrical waveguide created in a real metal deviates significantly from the PEC results [16]. However, it can be shown that a propagation mode can be achieved for a triangular array of cylindrical waveguides when the spacing between the waveguides is sufficiently small. Figure 4 shows the dispersion diagram of this supermode for a lattice constant of 420 nm, calculated by a finite element method. The metal is first described by a lossless Drude model, $\varepsilon = 1 - \omega_p^2/\omega^2$, in the calculations. The plasma frequency ω_p is taken as 1.425×10^{16} rad/s. This guided cylindrical mode has a real phase constant, β, larger than the wave number, k_0, supported by free space. The use of the lossless Drude model in the numerical simulations simplifies the identification of propagation modes as the propagation mode has a negligible attenuation constant. Simulations were then carried out using measured Ag dielectric constants [19] and the previous Drude model calculations as initial conditions, these supermodes also include a non-zero attenuation constant with a small correction to β. In each crystal period, the propagation mode is predominantly localized along the cylindrical sidewall. Due to the large spatial distribution of the mode, it is the most efficient to be excited by a spatially coherent light source. The calculations were carried out for square lattice 2-D periodic structures for the same hole radii and lattice constants as in triangular lattice structures, no such propagation modes have been observed.

Placing such a waveguide between two media, a cavity resonance is formed when

$$2\beta d + \angle r_c + \angle r_s = 2m\pi, \quad m \in Z \qquad (2)$$

where d is the thickness of the Ag film, $\angle r_c$ is the phase of reflection coefficients r_c at the interface of the waveguide and air, and $\angle r_s$ is that at the interface of the waveguide and glass substrate. This cavity resonance is essentially a weak Fabry-Perot interference that ultimately leads to a formation of standing wave inside the cylindrical air holes. The peak transmission due to the cavity resonance is nearly independent of the incident angle. Because of the propagation loss of the supermode, the cavity resonance becomes weaker with an increasing film thickness. The shortest cavity is formed when the thickness d equals to a quarter wavelength of the propagation mode. In this case, Eq. (2) is satisfied if one of the reflections coefficient possesses a π phase shift. Figure 4 shows that such a condition can be achieved only if the refractive index of the

NOTICE: This is the author's version of a work accepted for publication by Elsevier. Changes resulting from the publishing process, including peer review, editing, corrections, structural formatting and other quality control mechanisms, may not be reflected in this document. Changes may have been made to this work since it was submitted for publication. The definitive version has been published in Optics Communications, Vol. 283, Issue 20, Oct. 2010. DOI: 10.1016/j.optcom.2010.05.055

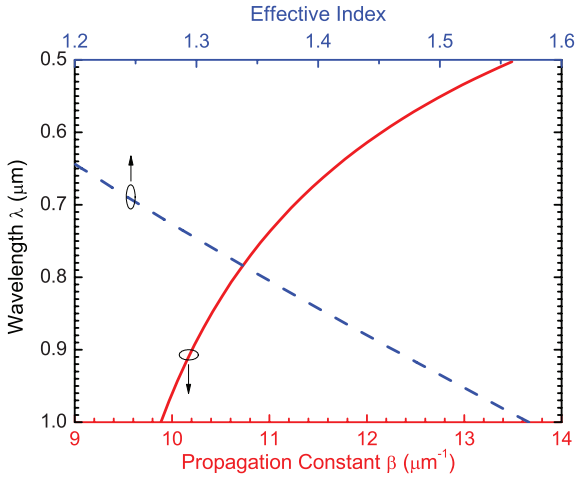

Figure 4: Dispersion diagram for super waveguide modes in a triangular array of cylindrical hollow waveguides, as shown in the inset. A lossless Drude model is assumed for the metallic medium in this calculation. The effective index of the supermode is also shown as a function of wavelength.

substrate is higher than 1.5. Increasing refractive index contrast could result in a sharper Fabry-Perot interference. The choice of Schott's N-SF6 glass, whose refractive index is about 1.8 at 800 nm [20], is designed to satisfy these requirements.

The insets of Fig. 2 show the calculated electric field components, E_x and E_z, on plasmonic crystals excited by a 30° p-wave incidence. The fields are plotted on a cross-section made along the $\Gamma - K$ direction. The modes are calculated by a 3D FDTD method with a Bloch-Floquet boundary condition applied to the primitive cell of plasmonic crystals. The electric fields highlight the differences between a cavity resonant mode and a planar surface mode. For planar surface modes, the field localizes along the interface of Ag and substrate. In comparison, the cavity resonant mode localizes the electric field inside the cylindrical air holes along the metal sidewall. The standing wave has a peak intensity near the high-index substrate and a valley near the low-index air interface, in agreement with the previous analysis. The spatial distribution of the supermode also indicates that it couples best with incident beam polarized in the $\Gamma - K$ direction. Experiments confirm that the cavity resonance is not observed for incident light linearly polarized in the $\Gamma - M$ direction.

Figure 3 shows that the planar surface mode and cavity resonant mode form an anti-cross near 20°. The energy gap formed between the two modes is 170 meV. This indicates a strong field overlap between the cavity resonant mode and planar surface mode. In comparison, we also conducted a number of measurements on periodically modified Ag films of a larger $600 - 650$ nm lattice, where planar surface modes on Ag-air and Ag-glass interfaces can be excited at the same wavelength for the same incident angle. For an Ag film of finite thickness, the inteaction of two surface modes leads to a spectral anti-cross. Fig. 5(a) shows the dispersion diagram for a periodically modified Ag film in 650 nm triangular lattice. The region of interest is highlight in circle and further examined in Fig. 5(b). Figure 5(b) shows the reflectance of the same structure for p-polarized incidence from the Ag side, measured for $25° - 45°$ at an interval of 1° and a 2 nm wavelength increment. The reflection spectra distinguishes two surface modes better than the transmission spectra [6]. The excitation of surface modes at both Ag-glass and Ag-air interfaces lead to a decrease of reflection. At 35°, an anti-crossing can be identified where two surface modes of an infinite metal would have intersect. However, the overlap of two planar surface modes is greatly diminished by the strong exponential decay of the field inside the metal film, which lead to an anti-cross of less than 20 meV. In contrast, the strong interaction between the cavity resonance and surface mode suggests the feasibility of converting between localized SPPs and extended, or long-range SPPs. This property can be utilized to improve the sensitivity of surface plasmon sensors. Oftentimes, the target analyte cannot distribute near the peak field strength of the planar surface modes. An increased sensitivity can be expected for resonance mediated by the cavity resonant mode as it exposes the electromagnetic field more towards the analyte.

4. Conclusions

In summary, the measurements and numerical models confirmed the existence of a cavity resonant mode in a periodically perforated metallic film. This resonance is due to the propagation mode in the cylindrical waveguide. However, this propagation mode differs from 1D slits, rectangular holes, or annular rings in that its existence relies partly on the periodic arrangement of circular holes. For an incident light with a linear polarization parallel to the plane of incidence and aligned to the $\Gamma - K$ orientation of plasmonic crystals, cavity resonances in circular air holes are observed besides the excitations of SPPs on the Ag-glass interface. The strong interaction between the cavity resonance and planar surface modes leads to an anti-cross spectral behavior. This could be exploited in the sensing applications to increase the device sensitivity.

The authors gratefully acknowledge the support from NSF CAREER ECCS-0846415 and DARPA Contract No. N66001-01-C-80345 for this work.

[1] T. W. Ebbesen, H. J. Lezec, H. F. Ghaemi, T. Thio, P. A. Wolff, Extraordinary optical transmission through sub-wavelength hole arrays, Nature 391 (1998) 667–669. doi:10.1038/35570.

[2] C.-Y. Chang, H.-Y. Chang, C.-Y. Chen, M.-W. Tsai, Y.-T. Chang, S.-C. Lee, S.-F. Tang, Wavelength selective quantum dot infrared photodetector with periodic metal hole arrays, Appl. Phys. Lett. 91 (16) (2007) 163107–3.
URL http://link.aip.org/link/?APL/91/163107/1

NOTICE: This is the author's version of a work accepted for publication by Elsevier. Changes resulting from the publishing process, including peer review, editing, corrections, structural formatting and other quality control mechanisms, may not be reflected in this document. Changes may have been made to this work since it was submitted for publication. The definitive version has been published in Optics Communications, Vol. 283, Issue 20, Oct. 2010. DOI: 10.1016/j.optcom.2010.05.055

[3] G. M. Hwang, L. Pang, E. H. Mullen, Y. Fainman, Plasmonic sensing of biological analytes through nanoholes, Sensors Journal, IEEE 8 (12) (2008) 2074–2079. doi:10.1109/JSEN.2008.2007663.

[4] L. Martín-Moreno, F. J. García-Vidal, H. J. Lezec, K. M. Pellerin, T. Thio, J. B. Pendry, T. W. Ebbesen, Theory of Extraordinary Optical Transmission through Subwavelength Hole Arrays, Physical Review Letters 86 (2001) 1114–1117. arXiv:arXiv:cond-mat/0008204, doi:10.1103/PhysRevLett.86.1114.

[5] N. Stefanou, A. Modinos, V. Yannopapas, Optical transparency of mesoporous metals, Solid State Communications 118 (2) (2001) 69 – 73. doi:DOI: 10.1016/S0038-1098(01)00038-2.
URL http://www.sciencedirect.com/science/article/B6TVW-42JRCX7-3/2/3b692d409235efbcf9752cf18389813e

[6] W. L. Barnes, W. A. Murray, J. Dintinger, E. Devaux, T. W. Ebbesen, Surface Plasmon Polaritons and Their Role in the Enhanced Transmission of Light through Periodic Arrays of Subwavelength Holes in a Metal Film, Phys. Rev. Lett. 92 (10) (2004) 107401–+. doi:10.1103/PhysRevLett.92.107401.

[7] F. Marquier, J.-J. Greffet, S. Collin, F. Pardo, J. L. Pelouard, Resonant transmission through a metallic film due to coupled modes, Optics Express 13 (2005) 70–+. doi:10.1364/OPEX.13.000070.

[8] M. Bai, N. García, Transmission of light by a single subwavelength cylindrical hole in metallic films, Appl. Phys. Lett. 89 (14) (2006) 141110–+. doi:10.1063/1.2358210.

[9] L. Pang, G. M. Hwang, B. Slutsky, Y. Fainman, Spectral sensitivity of two-dimensional nanohole array surface plasmon polariton resonance sensor, Appl. Phys. Lett. 91 (12) (2007) 123112–+. doi:10.1063/1.2789181.

[10] J. A. Porto, F. J. García-Vidal, J. B. Pendry, Transmission Resonances on Metallic Gratings with Very Narrow Slits, Phys. Rev. Lett. 83 (1999) 2845–2848. arXiv:arXiv:cond-mat/9904365, doi:10.1103/PhysRevLett.83.2845.

[11] Y. Chen, Y. Wang, Y. Zhang, S. Liu, Numerical investigation of the transmission enhancement through subwavelength hole array, Optics Communications 274 (2007) 236–240. doi:10.1016/j.optcom.2007.02.001.

[12] F. Wu, D. Han, X. Li, X. Liu, J. Zi, Enhanced transmission mediated by guided resonances in metallic gratings coated with dielectric layers, Optics Express 16 (2008) 6619–+. doi:10.1364/OE.16.006619.

[13] F. Yang, J. R. Sambles, Resonant transmission of microwaves through a narrow metallic slit, Phys. Rev. Lett. 89 (6) (2002) 063901. doi:10.1103/PhysRevLett.89.063901.

[14] K. J. K. Koerkamp, S. Enoch, F. B. Segerink, N. F. van Hulst, L. Kuipers, Strong influence of hole shape on extraordinary transmission through periodic arrays of subwavelength holes, Phys. Rev. Lett. 92 (18) (2004) 183901–183904.
URL http://link.aps.org/doi/10.1103/PhysRevLett.92.183901

[15] C. Rockstuhl, F. Lederer, T. Zentgraf, H. Giessen, Enhanced transmission of periodic, quasiperiodic, and random nanoaperture arrays, Appl. Phys. Lett. 91 (15) (2007) 151109. doi:10.1063/1.2799240.
URL http://link.aip.org/link/?APL/91/151109/1

[16] P. B. Catrysse, S. Fan, Propagating plasmonic mode in nanoscale apertures and its implications for extraordinary transmission, Journal of Nanophotonics 2 (1) (2008) 021790. doi:10.1117/1.2890424.
URL http://link.aip.org/link/?JNP/2/021790/1

[17] S. G. Tikhodeev, A. L. Yablonskii, E. A. Muljarov, N. A. Gippius, T. Ishihara, Quasiguided modes and optical properties of photonic crystal slabs, Phys. Rev. B 66 (4) (2002) 045102–.
URL http://link.aps.org/doi/10.1103/PhysRevB.66.045102

[18] Z. Ruan, M. Qiu, Enhanced Transmission through Periodic Arrays of Subwavelength Holes: The Role of Localized Waveguide Resonances, Phys. Rev. Lett. 96 (23) (2006) 233901–+. doi:10.1103/PhysRevLett.96.233901.

[19] P. B. Johnson, R. W. Christy, Optical constants of the noble metals, Phys. Rev. B 6 (12) (1972) 4370–4379. doi:10.1103/PhysRevB.6.4370.

[20] Schott, Inc., Optical glass: Data sheets (2009).
URL http://www.us.schott.com/advanced_optics/english/download/da

NOTICE: This is the author's version of a work accepted for publication by Elsevier. Changes resulting from the publishing process, including peer review, editing, corrections, structural formatting and other quality control mechanisms, may not be reflected in this document. Changes may have been made to this work since it was submitted for publication. The definitive version has been published in Optics Communications, Vol. 283, Issue 20, Oct. 2010. DOI: 10.1016/j.optcom.2010.05.055

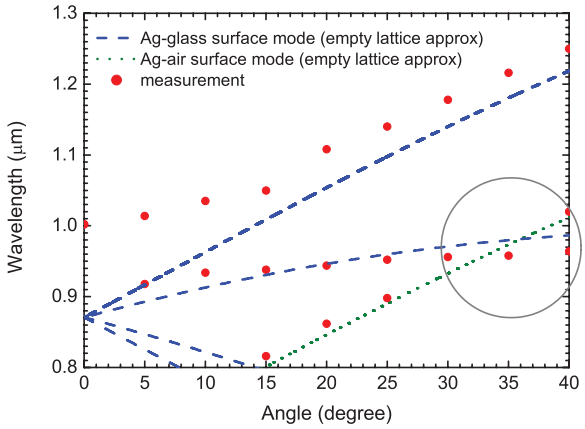

(a)

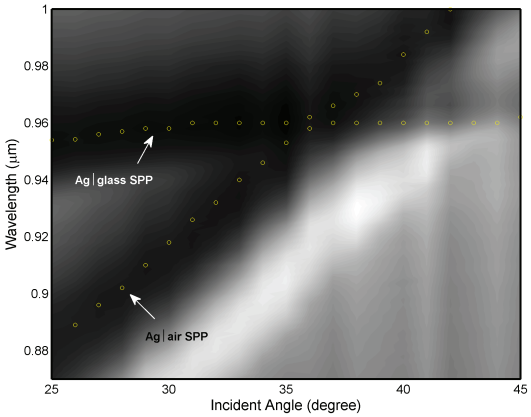

(b)

Figure 5: (a) Dispersion diagram of a 150 nm thick Ag film modified with a 2-D triangular lattice of air holes. The lattice constant is 650 nm. The circles are measured transmission peaks at a given incident angle for p-polarization. The dashed and dotted lines are results from semi-analytical models. The gray circle encloses the region where Ag-glass and Ag-air surface modes intersect and form an anti-cross. This is further shown in (b) where the reflectivity of the same structure was measured from the Ag side. The gray scale indicates the magnitude of the reflectance. Higher reflectivity is shown in white. The open circles in (b) locate the reflection minimums for a given incident angle.